Supramolecular Structure of Liquid-Crystalline Polyesters in Triclinic Cell

Domenico Acierno,[†] Simona Concilio,[‡] Luciano Di Maio,[‡] Pio Iannelli,*[,‡] Bernard Lotz,[§] and Paola Scarfato[†]

Dipartimento di Ingegneria dei Materiali e della Produzione, Università di Napoli, Piazzale Tecchio, I-80125 Napoli, Italy, Dipartimento di Ingegneria Chimica ed Alimentare, Università di Salerno, via Ponte Don Melillo, I-84084 Fisciano (Salerno), Italy, and Institut Charles Sadron (CNRS-ULP), 6 rue Boussingault, 67083 Strasbourg, France

Received September 20, 2001; Revised Manuscript Received December 5, 2001

ABSTRACT: We have analyzed the phase behavior of a series of liquid-crystalline polyesters bearing the *n*-alkoxy pendant group. For $n = 1-4$, this class of polymers shows a crystalline phase, called phase I, with a layered molecular packing and two chains per unit cell. For $n > 4$, a new molecular packing is observed. The new phase, called phase II, is characterized by the supramolecular assembly of 10−12 chains, each structurally independent of the others. This assembly is located in a large triclinic cell: in the case of **P**(5), the cell parameters are $a = 18.67$ Å, $b = 17.54$ Å, $c = 21.23$ Å, $\alpha = 111.1°$, $\beta = 81.7°$, and $\gamma = 105.5°$, with 10 chains per unit cell ($d_{calcd} = 1.23$ g cm^{-3}). The molecular packing of phase II is well-described in terms of a "fracture" of the layered molecular structure of phase I. This fracture is restored when samples are dipped into chlorinate solvents. The reason the packing fracture of phase I occurs is not clear: we believe that a complex balance between "packing incompatibility" of rigid chains and flexible side groups might be responsible for this phenomenon.

Introduction

Numerous parameters are involved in setting the ordered molecular packing of polymeric chains; this makes it difficult to predict a priori a universal quantitative correlation between chain structure and molecular packing.

It is well-known that, to have ordered crystalline materials, monomers and their sequence along the chain should fulfill specific requirements. For example, monomers should have highly symmetrical shapes and should be concatenated in an orderly fashion, giving rise to a well-defined "repetition unit". In the crystalline phase, the symmetry of monomers and chains is frequently retained by the space group: the more symmetric the shape of monomer and chain, the more symmetric the molecular packing. For instance, Isoda et al.[1] reported a trigonal unit cell, space group *P*3, for the β form of poly(*p*-xylylene). The unit cell contains 16 chains, with one of them being placed at the origin and adopting statistically the three orientations compatible with the *P*3 symmetry. The molecular packing is characterized by a waved allocation of chains, with the phenylene unit involved in both face-to-face and face-to-edge interchain contacts.

On the other hand, monomers can be appropriately designed to be asymmetric or copolymerized to give asymmetric molecular sequences to improve disorder in the solid state. These polymers are potentially amorphous, or if crystalline, they exhibit the less-ordered triclinic phase. In this case, only one or two chains are usually accommodated in the unit cell. However, large unit cells can be promoted by forcing several chains to aggregate in a supramolecular assembly, thus increasing the size of the repeating unit. This is the case for polymers bearing polar groups that promote strong interchain interactions.

Several examples of large crystalline structures have been reported for liquid-crystalline polymers (LCPs). Watanabe et al. reported the case of LCPs having the formula[2]

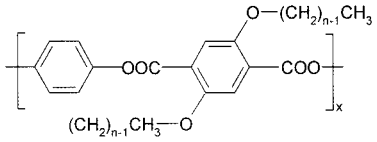

W(n)

for which they proposed a mesophasic structure with chains packed in a honeycomb fashion. In previous papers, we reported on the synthesis and characterization of LCPs having the formula[3,4]

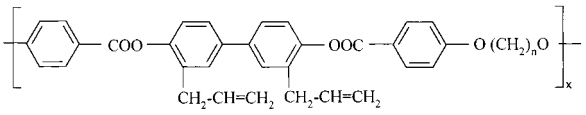

PA(n)

The incompatibility between the rigid aromatic core (mesogenic unit) and the flexible aliphatic pendant group promotes their separation in the molecular packing. This incompatibility results in the aggregation of chains into bundles having cylindrical symmetry.[4] For **PA**(10), bundles are packed in a hexagonal array with six chains per unit cell.

Recently, we reported on a class of LCPs having the formula[5,6]

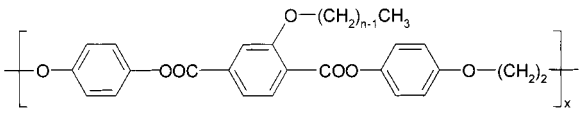

P(n) **n** = 1-8, 10

* Author to whom correspondence should be addressed. E-mail: piannelli@ unisa.it.
[†] Università di Napoli.
[‡] Università di Salerno.
[§] Institut Charles Sadron (CNRS-ULP).

10.1021/ma011652q CCC: $22.00
Published on Web 02/09/2002

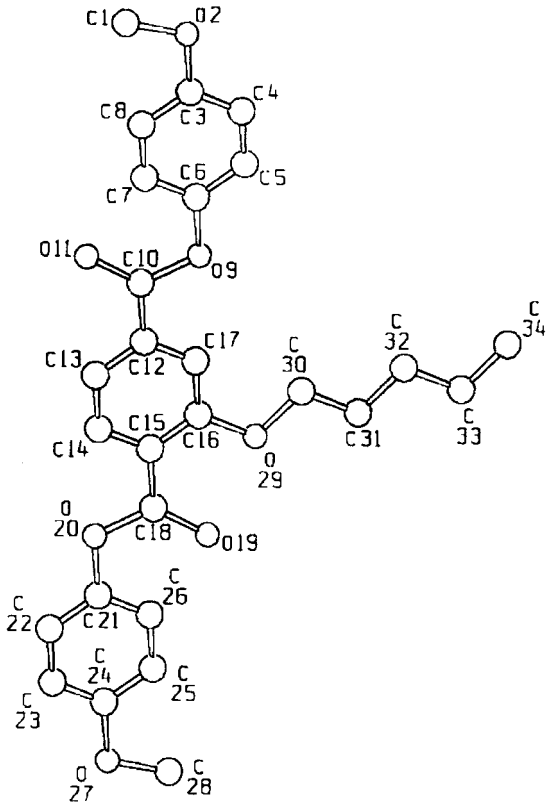

Figure 1. **P**(5) chain and atomic labels.

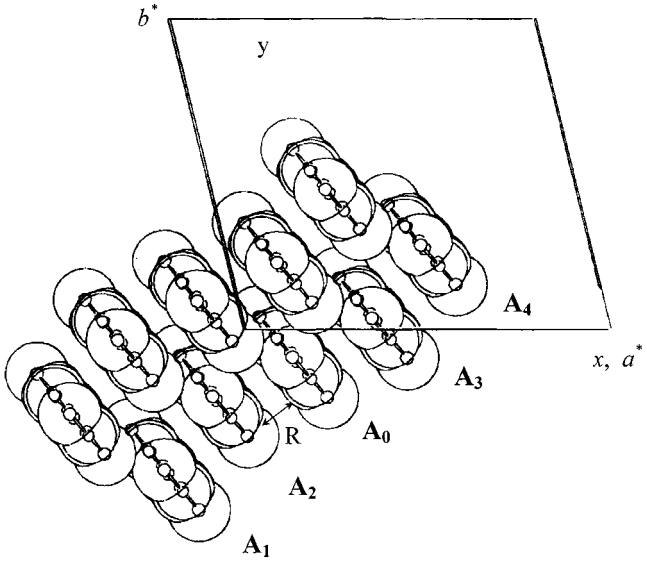

Figure 2. **P**(5) molecular assembly of 10 chains (viewed along the *c* axis).

These polymers are crystalline but have lower melting and isotropization temperatures relative to the same polymers without pendant groups.[7,8] The polymers **P**(*n*) with $n = 1-4$ exhibit a crystalline phase, called phase I, which was solved by the X-ray diffraction analysis of **P**(3).[6] The centrosymmetric triclinic cell contains two chains, which are layered and packed with side groups and chains separated from each other. **P**(*n*) with $n > 4$ exhibit a different crystalline phase, called phase II, with a unit cell much larger than that of phase I. In view of the triclinic unit-cell geometry and the large number of chains per cell [for example, 10 chains for **P**(5)], we could not elucidate the molecular packing of this phase.[5]

In the present paper, we report on the analysis and refinement of the molecular packing of phase II and discuss structural correlation between phases I and II.

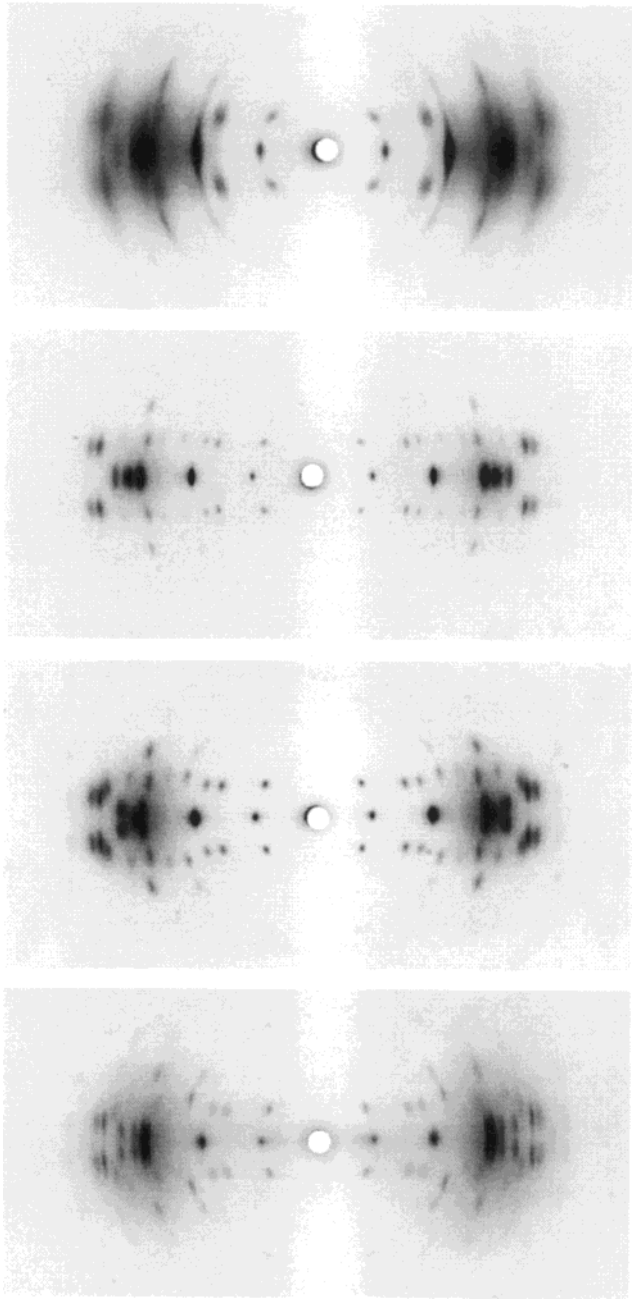

Figure 3. X-ray diffraction patterns of crystalline fiber samples of **P**(*n*) with $n = 1-4$ (phase I). From top to bottom: **P**(1), **P**(2), **P**(3), and **P**(4).

Table 1. Cell Parameters of Crystalline Phase I

polymer	*a* (Å)	*b* (Å)	*c* (Å)	α (°)	*β* (°)	*γ* (°)	d_{100} (Å)	ρ_{calcd}[a] (g/cm^3)
P(1)	14.03	6.43	20.1	134.7	117.8	84.9	11.48	1.28
P(2)	13.22	6.73	20.1	140.0	111.6	82.0	11.94	1.34
P(3)	13.20	6.48	20.1	138.3	110.9	80.8	12.15	1.37
P(4)	13.36	6.67	20.6	139.8	106.1	86.5	12.45	1.35
P(5)[b]	14.02	6.93	21.0	141.4	100.5	89.5	13.46	1.26

[a] Density calculated considering two chains per unit cell. [b] Crystalline phase I obtained by annealing CH_2Cl_2-swollen samples (phase III) at 160° for 2 h (see text).

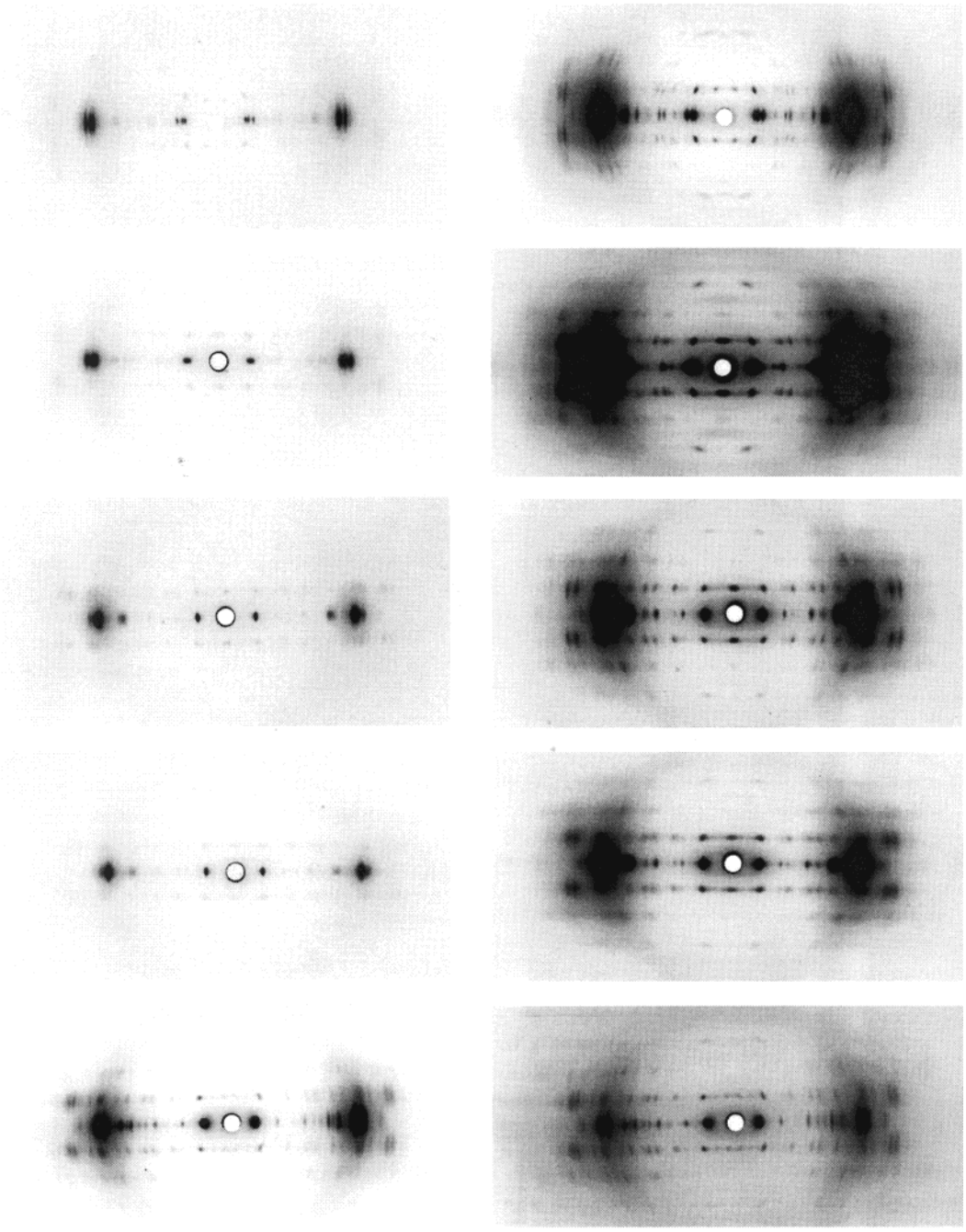

Figure 4. X-ray diffraction patterns of crystalline fiber samples of **P**(*n*) with $n = 5-8$, 10 (phase II) taken with two different exposure times: (left) 1 h and (right) 6 h. From top to bottom: **P**(5), **P**(6), **P**(7), **P**(8), and **P**(10).

Experimental Section

Polymer Synthesis. Polymers **P**(n) were synthesized by the condensation reaction of a mixture of the appropriate couple of substituted terephthalic acid chloride and 4,4′-dihydroxy-1,*n*-diphenoxyalkane, as outlined in refs 5 and 6.

Characterization. Fibers of **P**(*n*) were extruded from the nematic phase and cooled to room temperature. The average diameter of the fibers is 200−300 μm. Crystalline samples were obtained by annealing for 10 h at a temperature 10 °C below the melting temperature. Annealing was performed directly in the head of a Perkin-Elmer DSC-7 calorimeter.

Swollen samples were prepared by dipping fibers into the appropriate solvent for 2 days. Before use, swollen samples were removed from the solvent and left at room pressure and temperature for at least 1 day.

Diffraction spectra were recorded under vacuum by means of a cylindrical camera with a radius of 57.3 mm and with the X-ray beam direction perpendicular to the fiber axis (Cr Kα radiation, monochromatized by a flat graphite single-crystal monochromator). Fuji MS 2025 imaging plates and a Fuji Bio-imaging Analyzer System (model BAS-1800) were used to record diffraction patterns.

Structure Refinement Procedure

The "whole pattern" method[9,10] was applied to refine the crystalline molecular structure of **P**(5). This method is based on a least-squares fitting procedure to achieve the best match between two-dimensional experimental and calculated X-ray diffraction patterns. The parameters to be refined are of two kinds: (i) nonstructural ones, such as the crystalline size and the degree of crystallite orientation with respect to the fiber axis, and (ii) structural ones, such as the torsion angles defining the chain conformation and the cell parameters. The former parameters determine the shape, whereas the

Table 2. Cell Parameters[a] of Crystalline Phase II

polymer	*a* (Å)	*b* (Å)	*c* (Å)	α (°)	*β* (°)	*γ* (°)	ρ_{obs} (g/cm^3)	ρ_{calcd}/chain (g/cm^3)	number of chains
P(5)[a]	18.67	17.54	21.23	111.1	81.7	105.5	1.210	0.123	10
P(6)	19.95	18.12	21.2	95.5	87.6	111.9	1.191	0.112	11
P(7)	21.36	21.40	21.2	93.3	90.1	120.7	1.164	0.0981	12
P(8)	21.22	21.22	21.2	90.0	90.0	120.0	1.161	0.101	12
P(10)	24.13	21.89	21.2	95.3	91.8	121.1	1.156	0.0932	12−13

[a] As obtained from the structure refinement (this paper)

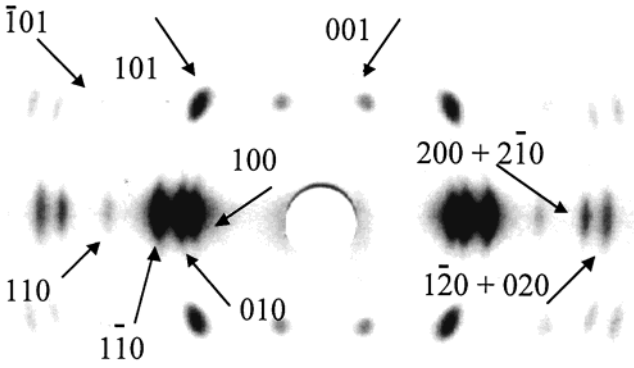

Figure 5. Schematic draft of the X-ray diffraction pattern of phase II for **P**(5).

Table 3. Observed and Calculated Lattice Spacings for Phase II, According to Cell Parameters Given in Table 2

	P(6)		**P**(7)		**P**(8)		**P**(10)	
hkl	d_{obsd} (Å)	d_{calcd} (Å)	d_{obsd} (Å)	d_{calcd} (Å)	d_{obsd} (Å)	d_{calcd} (Å)	d_{obsd} (Å)	d_{calcd} (Å)
100	18.50	18.51	18.37	18.36	18.38	18.38	20.48	20.58
010	16.70	16.75	18.37	18.36	18.38	18.38	18.50	18.59
$1\bar{1}0$	15.56	15.64	18.50	18.57	18.38	18.38	19.80	19.89
$11\bar{0}$	10.60	10.62	10.54	10.56	10.61	10.61	11.05	11.19
$2\bar{1}0$	9.71	9.78	10.62	10.68	10.61	10.61	12.00	12.05
200	−	9.23	9.08	9.18	9.19	9.19	−	10.29
$1\bar{2}0$	8.93	8.98	10.62	10.68	10.61	10.61	10.70	10.86
020	8.30	8.38	9.08	9.18	9.19	9.19	9.20	9.30
400	−	4.63	−	4.59	4.57	4.60	5.10	5.14
320	4.29	4.27	4.22	4.20	4.23	4.22	4.49	4.51
230	4.20	4.15	4.12	4.20	4.23	4.22	4.30	4.39
410	4.04	4.09	3.94	4.00	3.99	4.01	4.42	4.40
001	21.05	21.10	21.07	21.15	−	−	21.04	21.02
$\bar{1}01$	13.93	13.96	13.61	13.62	13.70	13.89	14.01	14.07
$\bar{1}01$	13.80	13.87	−	14.12	13.70	13.89	15.45	15.44

latter determine the diffraction intensity and the position of each diffraction spot.

In this article, the following nonstructural parameters are considered: (a) the main crystallite size (Δa, Δb, and Δc) taken along a direction parallel to the lattice axes (*a*, *b*, and *c*, respectively) and (b) the average angle (α_0) between the *c* lattice axis of the crystallites and fiber axis. α_0 is related to the degree of fiber orientation.

The structural parameters to be refined are (a) the lattice parameters defining the unit cell and (b) 12 parameters setting the molecular assembly of 10 chains according to Figures 1 and 2. To halve the number of independent chains, we placed a center of symmetry at the origin of cell, i.e., we assumed a centrosymmetric triclinic cell. The five independent chains are generated by starting from chain A_0, as depicted in Figure 2, by referring to a Cartesian frame with the $x-y$ plane coincident with the reciprocal a^*-b^* plane and the *x* and the *z* axes coincident with the reciprocal a^* axis and the crystallographic *c* axis, respectively. First, chain A_0 is placed in the $x-z$ plane with the center of mass at the origin; then, it is rotated by Φ_0 and shifted by X_0, Y_0, and Z_0. The other four chains are placed parallel to each other at an interchain distance of *R* and are shifted along *y* by Y_1, Y_2, Y_3, and Y_4 (for chains A_1, A_2, A_3, and A_4, respectively) with respect to chain A_0. Along the *z* axis, chains are shifted with respect to chain A_0 by Z_1 (A_3), $-Z_1$ (A_2), Z_2 (A_4), and $-Z_2$ (A_1). The entire set of five chains is rotated by Φ_1 about the origin. This structural model is only a coarse representation of the actual system. In the case of a supramolecular assembly of 10 chains, each one independent of the others, the true molecular structure can only be described as an average of similar but different molecular structures, with slight fluctuations of chain conformations as well

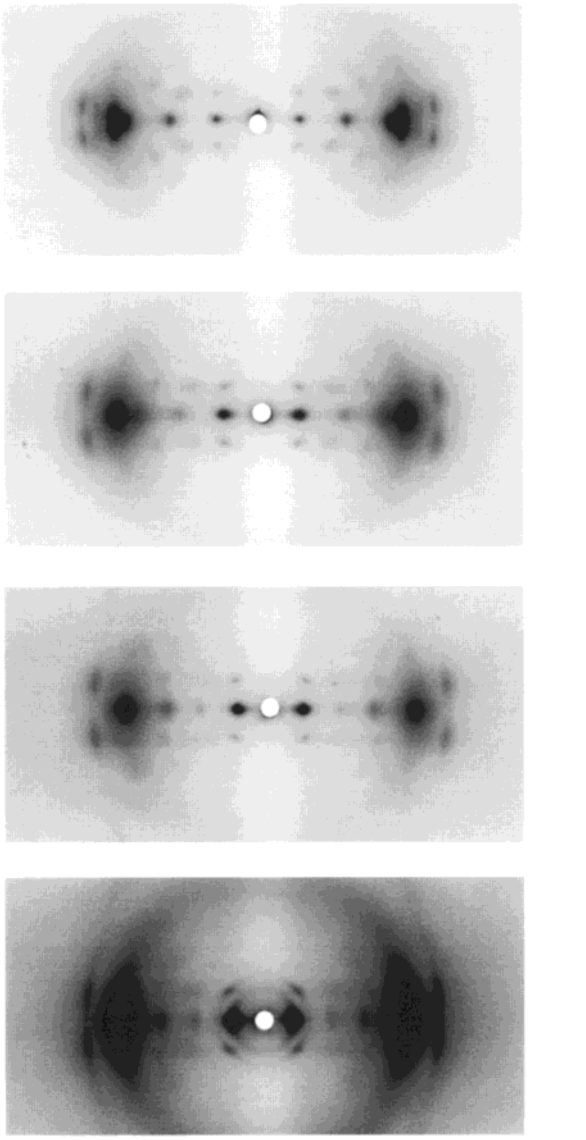

Figure 6. X-ray diffraction patterns of swollen fiber samples of **P**(*n*) (phase III). From top to bottom: **P**(3), **P**(5), **P**(8), and **P**(10).

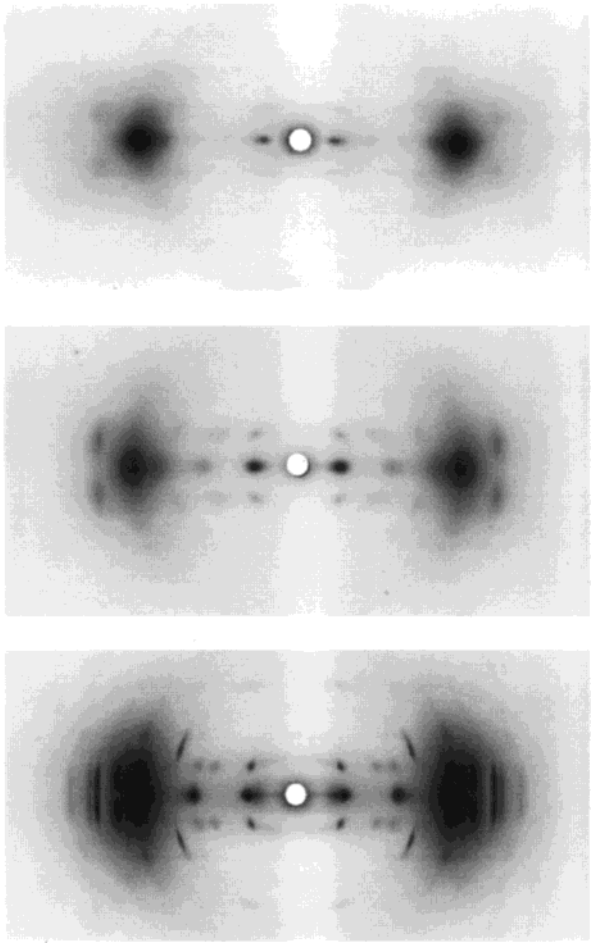

Figure 7. X-ray diffraction pattern of CCl_4- (top) and CH_2Cl_2- (middle) swollen samples of **P**(5) (phase III). Upon annealing at 140 °C for 30 min, the CH_2Cl_2-swollen sample undergoes a transition to phase I (bottom).

Table 4. Cell Parameters of Phase III (CH_2Cl_2 Swollen Samples)

polymer	a (Å)	b (Å)	c (Å)	α (°)	β (°)	γ (°)	d_{100}	ρ_{calcd}[a] (g/cm^3)
P(2)	15.20	6.68	21.2	140.0	123.4	70.8	12.50	1.23
P(3)	15.34	6.78	21.2	140.3	111.9	84.8	13.43	1.17
P(4)	15.27	6.81	20.8	140.1	104.3	91.5	13.88	1.18
P(5)	15.45	7.04	21.3	141.3	100.1	94.5	14.25	1.15
P(6)	17.98	6.78	21.1	139.8	103.9	91.7	16.42	1.04
P(7)	18.84	6.75	21.3	139.7	108.4	88.0	16.85	1.04
P(8)	19.66	6.64	21.2	138.8	112.0	86.1	17.08	1.06
P(10)	20.05	6.63	21.2	138.8	111.2	86.4	17.58	1.09

[a] Density calculated considering two chains per unit cell.

as of chain-to-chain register (rotation, distance, etc.). Of course, the X-ray diffraction technique employed in this investigation is not able to account for each of these different molecular assemblies. For this reason, the chain conformation could not be refined and was considered to be fully planar (Figure 1). Attempts at refining the chain conformation failed as a result of the divergence or the large fluctuation of the refining procedure.

The following structural parameters were taken as constant during the refinement procedure: bond lengths C−C = 1.54 Å, aromatic C=C = 1.40 Å, C=O = 1.23 Å, C−O = 1.43 Å; bond angles O−C−C = 109.5°, C−O−C = 109.5°, O−CO−C = 120°, aromatic C−C−C = 120°.

The isotropic thermal parameter was taken to be the same for all atoms (B_{iso} = 7.4 Å^2) and was not refined.

Table 5. Refined Parameters

structural parameters			
a = 18.67(4) Å	b = 17.54(2) Å	c = 21.23(1) Å	
α = 111.1(1)°	β = 81.7(4)°	γ = 105.5(2)°	Φ_0 = 256(4)°
X_0 = 0.168(1) Å	Y_0 = −2.65(1) Å	Z_0 = −1.128(3) Å	R = 3.93(1) Å
Y_1 = −2.04(2) Å	Y_2 = 1.98(6) Å	Y_3 = −2.34(3) Å	Y_4 = −2.12(5) Å
Z_1 = 0.19(3) Å	Z_2 = 7.56(1) Å		
Φ_1 = 54.9(1)°			

nonstructural parameters			
Δa = 120(8) Å	Δb = 113(4) Å	Δc = 73.9(5) Å	α_0 = 5.79(4)°

To reduce the number of atoms, hydrogen atoms were not included in the calculation. Because of the random insertion of the terephthaloyl unit along the chain, as a result of the synthetic route, two pentyl units were taken into account, in mirror symmetry relative to a plane perpendicular to the terephthaloyl unit. As a consequence, the occupancy factor of 0.5 was imposed on each pentyl unit.

Following the standard procedure, a constraint was imposed on the chain backbone during the refinement, i.e., the chain length was required to match the c axis length.

Discussion

P(*n*) Phase Behavior. In previous investigations,[5,6] the polymers **P**(*n*) were shown to be semicrystalline polymers with two different crystalline phases at room temperature depending on the length of the side chains: phase I for $n = 1-4$ and phase II for $n = 5-10$.

The molecular packing of phase I was solved,[6] and the polymeric chains were found to pack in a centrosymmetric triclinic cell with two chains per unit cell. The structure is a layered one with the rigid chains and the flexible side groups segregated in layers. The X-ray diffraction fiber patterns of these polymers are shown in Figure 3. The cell parameters of phase I, for $n = 1-4$, are listed in Table 1.[6] The d_{100} spacing corresponding to the layer width depends little on the length of the side group, in agreement with the folded conformation of these side groups, oriented nearly parallel to the chain backbone. From a morphological standpoint, the most interesting feature is the slight tilt of the crystallites with respect to the fiber axis (tilting about the [100] direction), which is not observed in the case of phase II.

Phase II exhibits a much larger unit cell. Its triclinic nature is revealed by a careful analysis of the diffraction patterns (Figure 4) and the absence of extinction conditions. Particularly interesting are the position and relative movements of the six reflections at low diffraction angle, indexed as 100, 010, $1\bar{1}0$, 110, 001, and 101 (see Figure 5). For the sequence **P**(5)−**P**(10), reflection 001 moves to the meridian, which is reached for $n = 7$ and 8. At the same time, the four equatorial reflections get closer to each other and finally merge to form a single spot for $n = 7$ and 8, which would suggest an apparently hexagonal lattice. For $n = 10$, the hexagonal lattice is disrupted, with the 001 reflection away from the meridian and the equatorial reflections again separated, this time into two spots.

The cell parameters of phase II were evaluated by fitting the 15 most intense reflections in the diffraction patterns. The resulting values are given in Table 2, and the calculated and observed lattice spacings are compared in Table 3. Following common practice, the number of chains per unit cell was obtained by dividing

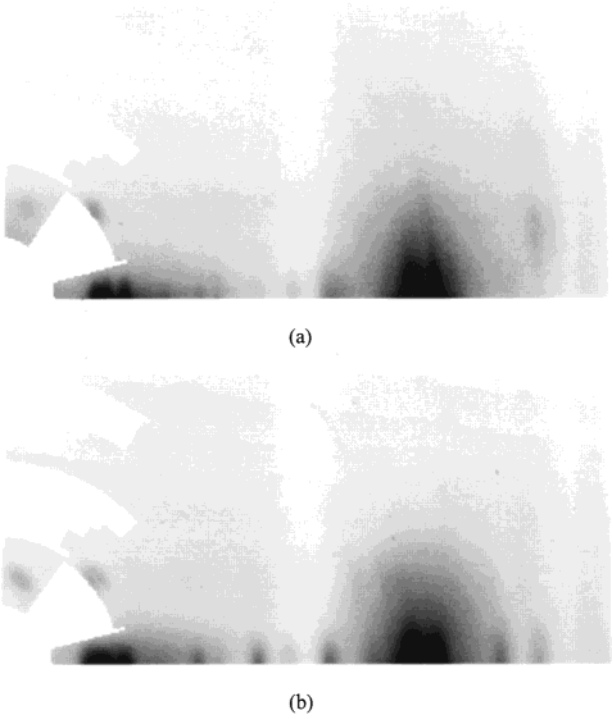

Figure 8. (a) Observed and (b) calculated X-ray diffraction pattern of **P**(5). Only one-quarter of the pattern is shown.

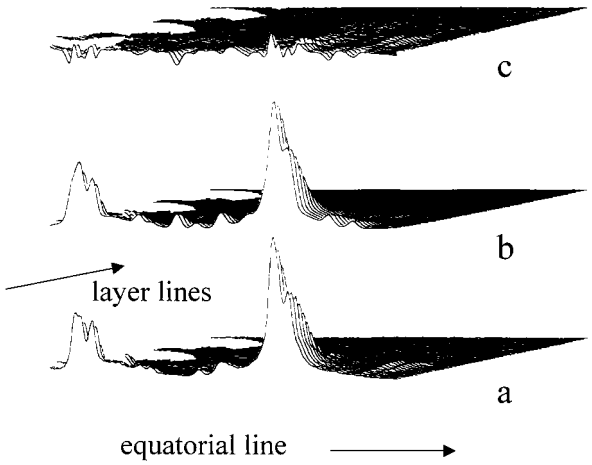

Figure 9. Three-dimensional representation of X-ray diffraction pattern of **P**(5) (same data as Figure 8): (a) observed, (b) calculated according to this article's approach, (c) difference between parts a and b.

the observed density by the calculated density for a single chain: the number of chains increases with n, going from an estimated 10 chains for **P**(5) to 12−13 chains for **P**(10). The figures must remain approximate, given the uncertainties associated with the experimental densities (linked with crystallinities).

The high number of independent chains per unit cell is unusual for polymeric materials: the packing symmetry is low, with numerous independent chains in the repeating unit, but the crystalline state is very well-developed, as indicated by the rich and well-resolved diffraction patterns. In other words, it seems that numerous chains are assembled together to give a stable and ordered supramolecular aggregate. We believe that the insertion of a single pendant group might be responsible for such supramolecular organization, because of the reduction of chain symmetry and the incompatibility between the rigid character of the chains and the flexible nature of the side group. A plausible, realistic model for this supramolecular packing is discussed in the next section.

The **P**(n) polymers are not soluble in common organic solvents at room temperature, but they swell when dipped into some chlorinate solvents, such as methylene chloride or carbon tetrachloride. As a result of the swelling, reorganization of the molecular packing takes place, and a new phase appears, called phase III, for methylene chloride-swollen samples. X-ray diffraction patterns of phase III resemble very much those of phase I but display fewer and broader diffraction spots; furthermore, the 100 reflection is located at a lower angle (Figure 6).

To illustrate the complex phase behavior of swollen fiber samples of **P**(n), two diffraction patterns of phase III are shown in Figure 7 for **P**(5). In Figure 7a, the diffraction pattern of a **P**(5) fiber treated with carbon tetrachloride displays a spot at an even lower angle than that for a sample swollen in methylene chloride (Figure 7b).

The cell parameters of phase III were refined by fitting the eight strongest diffraction spots, indexed as 100, 200, 300, 010, 001, 101, $0\bar{1}1$, and $\bar{1}11$. The resulting unit-cell parameters are given in Table 4. In view of the similarities in the diffraction spectra of the two phases, the layered molecular structure of phase I appears to be present in phase III as well. This inference is supported by the transformation of phase III into phase I when swollen samples of **P**(2), **P**(3), and **P**(4) are annealed for a few minutes. For $n > 5$, phase III reverts after annealing to phase II. This transformation indicates that the solvent-induced structural modifications are reversible and that phase II, despite its very different unit cell, is structurally close to phase III and, consequently, to phase I (see next section). **P**(5) corresponds to a transition in the series: by swelling, phase II transforms into phase III, and then, by annealing, phase III undergoes a transition into phase I (Figure 7c). In this case, phase II can be restored only by crystallization from the melt.

The overall phase behavior is summarized in the following sketches

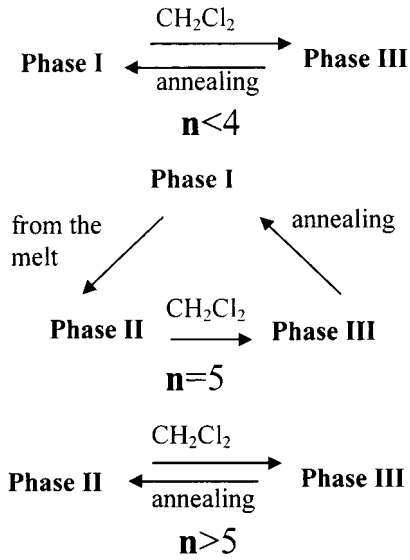

Structure Analysis and Refinement of Phase II. Because of the formation of a pseudohexagonal structure, several diffraction spots in the pattern of phase II

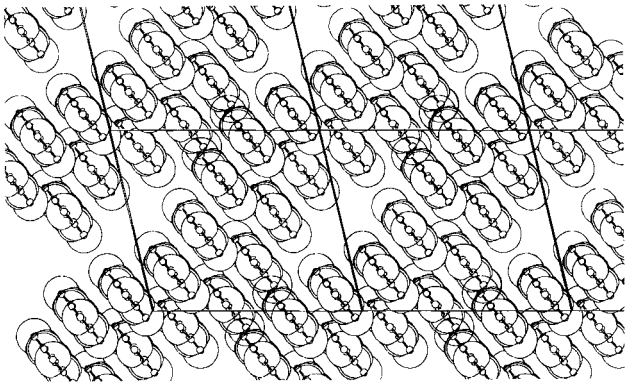

Figure 10. Molecular packing of **P**(5) in phase II. The empty space between chains is that available for the pendant side groups (not shown in the figure).

merge to some extent going from **P**(5) to **P**(10), with quite complete overlap occurring for $n = 7$ and 8. For **P**(5), reflections are well separated and identifiable in the pattern, thus providing more information for the structural refinement. Consequently, **P**(5) is analyzed as the representative term of the series.

To carry out a structure analysis, a structural model must be used. Previous investigations have shown that side groups promote the organization of several chains in bundles, creating a kind of amphiphilic structure.[4] This model can be considered for **P**(5) also, as it is compatible with 10 chains per unit cell. The validity of this model must be tested by comparing calculated and experimental diffraction patterns.

In the crystalline solid state, atoms are preferentially located on some specific crystallographic planes, giving rise to an ordered distribution of electron density in space. Diffraction from these planes is strong when no extinction occurs or when the contributions of the atoms to the diffraction are in phase. In the case of **P**(5), the strongest equatorial reflections are 100, 010, and $1\bar{1}0$ at low angles and 320, 230, and 410 at high angles. Particularly strong is reflection 320 with a 4.32-Å *d* spacing: this suggests a high density of atoms in the corresponding crystallographic plane.

The strong reflection 320 with the 4.32-Å *d* spacing is compatible with an extended layered packing. The layer model, built up as indicated in the Experimental Section, is tested by moving the five independent chains and rotating the whole set about the center of mass. Because of the large number of independent atoms (200, keeping in mind that hydrogen atoms are not included), only a limited number of structural parameters can be refined during the analysis. These parameters are reported in Table 5, as obtained for the best fit of the experimental data. The calculated and observed diffraction spectra are compared in Figures 8 and 9. The packing of the chains, as seen along the *c* axis direction, is shown in Figure 10. The intensity of the strongest reflections and the atomic coordinates are given in Tables 6 and 7, respectively.

The major feature of this structure is the layered organization, which very much resembles that of phase I. The transition from phase I to phase II might result from a "packing fracture" in the extended layer of phase I. This hypothesis is also substantiated by the formation of phase III when samples are dipped into methylene chloride: the packing fracture is repaired by the solvent as a result of the increased chain mobility. After annealing, the packing fracture reversibly reoccurs and phase III transforms into phase II. The only molecule that has a different behavior is **P**(5): by annealing, the packing fracture is definitively repaired and phase III undergoes transition to phase I. Phase II is restored only upon recrystallization from the melt.

Table 6. Calculated Integrated Intensities of the Strongest Diffraction Spots as Obtained the Structure Refinement

hkl[a]	I_{calcd}[b]	hkl[a]	I_{calcd}[b]	hkl[a]	I_{calcd}[b]
320	100.0	220	6.4	$00\bar{2}$	4.4
410	36.6	$0\bar{1}0$	6.3	$\bar{4}\bar{2}1$	4.1
230	36.1	$\bar{3}\bar{1}1$	5.7	$\bar{1}30$	3.4
400	12.3	$2\bar{2}0$	4.7	$\bar{4}01$	3.4
510	8.2	330	4.6	$\bar{1}00$	3.3
500	7.5	$1\bar{1}0$	5.2	$\bar{2}41$	3.0

[a] Bragg indices. [b] Calculated integrated intensities I_{calcd} are normalized to the maximum intensity peak of 100. Only reflections with $I_{calcd} > 3.0$ are given. Intensity is corrected for the Lorentz factor.

Table 7. Refined Atomic Fractional Coordinates of Molecule A_0[a]

atom	*x*	*y*	*z*
C1	0.1046	−0.0870	−0.1296
O2	0.1421	−0.1558	−0.1795
C3	0.1421	−0.1558	−0.2520
C4	0.1735	−0.2132	−0.3065
C5	0.1735	−0.2132	−0.3724
C6	0.1421	−0.1558	−0.3839
C7	0.1108	−0.0984	−0.3294
C8	0.1108	−0.0984	−0.2635
O9	0.1421	−0.1557	−0.4564
C10	0.1046	−0.0870	−0.4548
O11	0.0721	−0.0274	−0.3906
C12	0.1045	−0.0869	−0.5273
C13	0.0732	−0.0295	−0.5388
C14	0.0732	−0.0295	−0.6047
C15	0.1045	−0.0869	−0.6592
C16	0.1359	−0.1443	−0.6477
C17	0.1358	−0.1442	−0.5817
C18	0.1045	−0.0869	−0.7318
O19	0.1370	−0.1464	−0.7959
O20	0.0670	−0.0181	−0.7302
C21	0.0670	−0.0181	−0.8027
C22	0.0356	0.0393	−0.8142
C23	0.0356	0.0393	−0.8801
C24	0.0670	−0.0181	−0.9346
C25	0.0983	−0.0755	−0.9230
C26	0.0983	−0.0754	−0.8570
O27	0.0670	−0.0181	−1.0071
C28	0.1046	−0.0869	−1.0570
O29	0.1704	−0.2075	−0.7076
C30	0.2006	−0.2629	−0.6811
C31	0.2351	−0.3261	−0.7409
C32	0.2653	−0.3814	−0.7144
C33	0.2998	−0.4446	−0.7743
C34	0.3300	−0.5000	−0.7478

[a] See Figure 2

Conclusion

We have analyzed the complex phase behavior of **P**(*n*). For $n > 4$, polymers **P**(*n*) exhibit a molecular packing characterized by the supramolecular assembly of 10−12 chains that are structurally independent. This assembly is located in a large triclinic cell that displays long-range order.

Numerous examples of large molecular packing have been reported in the literature and are characterized by two opposite situations: (i) highly regular and symmetric chains and high packing symmetry with long-range order and (ii) irregular chains (i.e., with

pendant groups) and low packing symmetry with short-range order. In the latter case, few chains are accommodated in the unit cell. To our knowledge, the case of **P**(*n*) is unique because of the asymmetric chains with pendant groups and low packing symmetry (triclinic cell), but well-developed long-range order and numerous independent chains per unit cell.

The phase behavior of **P**(*n*) can be understood on the basis of the structural model described in the previous sections: phase II is the result of a fracture of the layered molecular structure of phase I, which involves a group of 10−12 chains, depending on *n*. In other words, this assembly of chains retains the local layered structure and rotates as a whole about its center of mass. The consequence is a triclinic unit cell with the molecular assembly at the origin and well-developed long-range order.

The reason the packing fracture of phase II leads to more stable packing compared to that of phase I is not clear. It is observed, however, that the "packing incompatibility" between the rigid chains and flexible side groups, which increases with side-group length, is responsible for this behavior.

Acknowledgment. Support from the Università degli Sudi di Salerno in partially financing this research project is gratefully acknowledged

References and Notes

(1) Isoda, S.; Tsuji, M.; Ohara, M.; Kawaguchi, A.; Katayama, K.-I. *Polymer* **1983**, *24*, 1155.
(2) Watanabe, J.; Sekine, N.; Nematsu, T.; Sone, M.; Kricheldorf, H. R. *Macromolecules* **1996**, *29*, 4816.
(3) Caruso, U.; Iannelli, P.; Roviello, A.; Sirigu, A. *J. Polym. Sci. B: Polym. Phys.* **1998**, *36*, 2371.
(4) Acierno, D.; Di Maio, L.; Iannelli, P. *J. Polym. Sci. B: Polym. Phys.* **1999**, *37*, 1601.
(5) Caruso, U.; Iannelli, P.; Pragliola, S.; Roviello, A.; Sirigu, A. *Macromolecules* **1995**, *28*, 6089.
(6) Iannelli, P.; Pragliola, S.; Roviello, A.; Sirigu, A. *Macromolecules* **1997**, *30*, 4247.
(7) Antoun, S.; Lenz, R. W.; Jin, J. I. *J. Polym. Sci. B: Polym. Phys.* **1981**, *19*, 1901.
(8) Uryu, T.; Kato, T. *Macromolecules* **1988**, *21*, 378.
(9) Iannelli, P. *Macromolecules* **1993**, *26*, 2303.
(10) Iannelli, P. *J. Appl. Crystallogr.* **1994**, *27*, 1055.

MA011652Q